

**SYNTHESIS, CHARACTERIZATION, AND
CYTOTOXICITY EVALUATION OF
MAGNESIUM-DOPED BIPHASIC CALCIUM
PHOSPHATE (Mg-BCP) POWDERS**

BALLOUZE RAMA

UNIVERSITI SAINS MALAYSIA

2021

**SYNTHESIS, CHARACTERIZATION, AND
CYTOTOXICITY EVALUATION OF
MAGNESIUM-DOPED BIPHASIC CALCIUM
PHOSPHATE (Mg-BCP) POWDERS**

by

BALLOUZE RAMA

**Thesis submitted in fulfillment of the requirements
for the degree of
Master of Science**

October 2021

ACKNOWLEDGEMENT

Nothing could ever start or be accomplished without the support of many good souls. Therefore, I would like to express my sincere gratitude toward my main supervisor Dr. Ooi Jer Ping for his continuous guidance at every step, his precious help in developing my skills, and his constant encouragement during hard moments. I am very grateful for his endless support for me to survive this journey, it has been a great proud to work under his supervision. I am also grateful to my co-supervisors; Dr. Shah Rizal Kasim and Dr. Nor Aini Binti Saidin, for their kind guidance and support throughout this project. Many thanks to Mr. Muhammad Hanif Bin Marahat for sharing with me his expertise in the field of material synthesis. My appreciation extends to all AMDI's staff (especially the integrative medicine and oncology clusters) for helping me use the labs' equipment and instruments. Moreover, I would like to acknowledge the USM short-term grant for the financial support of this project.

I am also deeply thankful to my laboratory mates at ARC, especially Dr. Ibrahim D. T. Al Deeb, Mohamed Salih Elnour, Anan A Ishtiah, Julia Joseph, and Khor Kang Zi, who improved my lab work with their brilliant ideas and kind help. No words can describe my gratitude to my beloved husband and best friend Orwa and my loving parents Elias and Bassema who always believed in me and granted their unlimited support for my personal plans. Last, but not least, my profound gratitude and endless love are for my sister; Ruba, my brother; Rami and his family; Marie, Elias, and Andro, and my friends from my home country; Heba, Alaa, Riham, Khaled, George, Dema, who have been the constant source of energy and inspiration during this journey.

Finally, I would like to express my sincere love for my loving home, my sunshine, Syria.

TABLE OF CONTENTS

ACKNOWLEDGEMENT	ii
TABLE OF CONTENTS	iii
LIST OF TABLES	vii
LIST OF FIGURES	viii
LIST OF SYMBOLS AND UNITS	xi
LIST OF ABBREVIATIONS	xiii
LIST OF APPENDICES	xvi
ABSTRAK	xvii
ABSTRACT	xix
CHAPTER 1 INTRODUCTION	1
1.1 History of Bone Substitutes.....	1
1.2 Calcium Phosphate Bioceramics as Bone Substitutes.....	2
1.3 Magnesium Doped Biphasic Calcium Phosphate: A Better Bone Substitute ..	4
1.4 Problem statement	6
1.5 Objectives of the study	7
CHAPTER 2 LITERATURE REVIEW	8
2.1 Bone Tissue and the Bone Repair Process	8
2.2 Bone Grafting Materials	10
2.3 Calcium Phosphates	12
2.4 Mg-doping of CaPs towards Developing Mg-BCP.....	17
2.5 Mg-BCP Synthesis Routes	22
2.6 <i>In Vitro</i> and <i>In Vivo</i> Biocompatibility of Mg-BCP	28
2.6.1 The Apatite-Forming Ability of Mg-BCP.....	28
2.6.2 Cytocompatibility and <i>In Vivo</i> Compatibility of Mg-BCP	32

CHAPTER 3	MATERIALS AND METHODS	35
3.1	Overview of the Research Methods	35
3.2	Mg-BCP Powder Synthesis via Wet Chemical Precipitation	37
3.2.1	Materials and Equipment	37
3.2.2	Wet Chemical Precipitation Synthesis of Mg-BCP Powder	37
3.3	Sample Characterization	41
3.3.1	Equipment	41
3.3.2	XRD Analysis	41
3.3.3	SEM-EDX Analysis	42
3.3.4	FT-IR Analysis	43
3.4	Cell Culturing	43
3.4.1	Materials and Reagents Preparation	43
3.4.2	Cells Resuscitation	45
3.4.3	Maintaining Cell Culture	46
3.4.4	Subculturing of hFOB 1.19 Cell Line	47
3.4.5	Counting hFOB 1.19 Cells Using Trypan Blue Dye Exclusion Method	48
3.4.6	Cryopreservation of hFOB 1.19 Cell Line	48
3.5	Cytotoxicity Evaluation of Mg-BCP Powders	49
3.5.1	Materials and Equipment	50
3.5.1(a)	Sample Preparation	50
3.5.1(b)	Reagents Preparation for NR Assay	51
3.5.2	Optimization of Cytotoxicity Assays	51
3.5.2(a)	Cell Seeding Number	51
3.5.2(b)	DMSO Volume and Absorbance Wavelength	52
3.5.3	MTT Assay and Analysis	53
3.5.4	NR Assay and Analysis	56
3.6	ALP Activity Assay	57

3.6.1	Materials and Equipment	58
3.6.2	Sample and Reagents Preparation for ALP assay	58
3.6.3	Optimization of ALP Activity Assay	59
	3.6.3(a) Cell Seeding Number.....	59
	3.6.3(b) Incubation Duration and Temperature.....	60
	3.6.3(c) Protein Concentration	61
3.6.4	ALP Activity Assay and Analysis.....	62
3.7	Cell Morphological Observation	67
3.8	Statistical Analysis	68
	3.8.1 Prediction of IC ₅₀ Value of Mg-BCP Powders Using a Nonlinear Regression Model.....	68
	3.8.2 Statistical Analysis of MTT and NR Assay	69
	3.8.3 Statistical Analysis of ALP Activity Assay	70
CHAPTER 4	RESULTS.....	71
4.1	Samples Synthesis	71
4.2	Samples Characterization	72
	4.2.1 XRD Analysis	72
	4.2.2 SEM-EDX Analysis	73
	4.2.3 FT-IR Analysis.....	77
4.3	Cytotoxicity Evaluation.....	80
	4.3.1 MTT Assay Analysis.....	80
	4.3.2 NR Assay Analysis.....	84
4.4	ALP Activity Assay Analysis	86
4.5	Cell Morphological Observation	88
CHAPTER 5	DISCUSSION	91
5.1	Mg-BCP – A Potential Synthetic Bone Substitute.....	91
5.2	Mg-BCP Powders Synthesis and Characterization	92
5.3	<i>In Vitro</i> Biocompatibility of Mg-BCP Powders.....	101

CHAPTER 6	CONCLUSION AND FUTURE RECOMMENDATIONS...	109
6.1	Conclusion.....	109
6.2	Limitations of This Study.....	110
6.3	Recommendations for Future Research	111
	REFERENCES.....	113
	LIST OF PUBLICATIONS.....	136
	APPENDICES	
	LIST OF PUBLICATIONS	

LIST OF TABLES

	Page
Table 2.1	The weight percentage (wt%) composition of inorganic phases of adult human calcified tissues (Kannan et al., 2008)..... 18
Table 2.2	The methods, precursors, and synthesis parameters that were used to synthesize Mg-BCP powders.25
Table 2.3	Ion concentration in blood plasma, SBF*, HBSS*, and DMEM*.....29
Table 3.1	The precursors and reagents that were involved in Mg-BCP synthesis.37
Table 3.2	The molecular weight, the molar concentration, the volume of solvent, and the mass of the precursors involved in the Mg-BCP synthesis process.38
Table 3.3	The equipment used in Mg-BCP and BCP characterization experiments.41
Table 3.4	Reagents list for the cell culture experiments.44
Table 3.5	Equipment list for the cell culture experiments.45
Table 3.6	Reagents list for cytotoxicity assays.50
Table 3.7	The kits list for the ALP activity assay.58
Table 4.1	The quantification analysis of BCP and MgBCP..... 73
Table 4.2	The elemental composition of Mg-BCP and BCP estimated by EDX analysis..... 76
Table 4.3	The functional groups that were found in the Mg-BCP and BCP FT-IR spectrum. 78
Table 5.1	A comparison between SEM images for BCP and Mg-BCP.....98

LIST OF FIGURES

	Page
Figure 2.1	The phase diagram of HA and TCP. 16
Figure 2.2	The crystal structure of (a) HA and (b) β TCP where Mg preferentially accommodates in the Ca(4) and Ca(5) site (red in color) of the β TCP lattice (Ballouze et al., 2021; Kannan et al., 2008).21
Figure 2.3	SEM images of BCP, 0.5, and 1 wt% substituted Mg-BCP after 1, 2, and 4 weeks soaking in HBSS (Kim et al., 2012).31
Figure 2.4	Images after 1 and 2 months of <i>in vivo</i> implantation of hAT-MSCs alone (left) or with Mg-BCP micro scaffolds (right) in a skull of an immunodeficient mouse (Kim et al., 2013).33
Figure 3.1	The flowchart of the project's methodology.36
Figure 3.2	Mg-BCP synthesis via wet precipitation method.38
Figure 3.3	The calcination profile for Mg-BCP and BCP powders.40
Figure 3.4	The plate set up in the MTT and NR assays where Mg-BCP doses were added to B, C, and D rows (in the grey colored wells), and BCP doses were added to E, F, and G rows (in the black colored wells).55
Figure 3.5	The plate design in the ALP assay where Mg-BCP with the doses of 0, 50, and 200 μ g/mL were added to B2, C2, and D2 wells, respectively.63
Figure 3.6	The plate set up in the protein concentration assay where; the white colored wells in C2 and C3 contains the BSA standard dilutions; the light grey-colored wells in C5 contains the blank (DPBS); the light grey-colored wells in C6 contains the untreated cell lysate; the dark grey-colored wells in C7, and C8 contains the cell lysate treated with Mg-BCP; the black-colored wells in C10 and C11 contains the cell lysate treated with BCP.65

Figure 3.7	The plate set up in the ALP activity assay where; the white-colored wells in C2 and C3 contains the phenol standard dilutions; the light grey-colored wells in C5 contains the blank (DPBS); the light grey-colored wells in C6 contains the untreated cell lysate; the dark grey-colored wells in C7, and C8 contains the cell lysate treated with Mg-BCP; the black-colored wells in C10 and C11 contains the cell lysate treated with BCP.	66
Figure 4.1	The appearance of the (a) Mg-BCP and (b) BCP synthesized powders.	71
Figure 4.2	The XRD result analysis of BCP and MgBCP sample.	72
Figure 4.3	SEM images showing (a) the overall structure and agglomeration for Mg-BCP powder at 5000x magnifying power, (b) the surface texture for Mg-BCP powder at 10000x magnifying power, (c) the overall structure and agglomeration for BCP powder at 5000x magnifying power, and (d) the surface texture for BCP at 10000x magnifying power.	74
Figure 4.4	SEM images showing the size and shape of particles of Mg-BCP powder at (a) 100000x and (b) 120000x magnifying power, and the size and shape of particles of BCP powder in (c) 100000x and (d) 120000x magnifying power, respectively.	75
Figure 4.5	The elemental composition for Mg-BCP and BCP in the EDX spectrum.	76
Figure 4.6	The EDX mapping for (a) Mg-BCP and (b) BCP.	77
Figure 4.7	The FT-IR spectrum for Mg-BCP and BCP.	78
Figure 4.8	The cytotoxicity effects of Mg-BCP and BCP at (a) 24, (b) 48, and (c) 72 h against hFOB 1.19 cells using MTT assay (mean \pm SD, n = 3). Data marked with * have a significant difference from the control group (p < 0.05).	81
Figure 4.9	The nonlinear regression model based on the sigmoidal dose-response curve (variable slope) of Mg-BCP and BCP with interpolated IC ₅₀ and 95 % confidence band.	83

Figure 4.10	The cytotoxicity effects of Mg-BCP and BCP at (a) 24, (b) 48, and (c) 72 h against hFOB 1.19 using NR assay (mean \pm SD, n = 3). Data marked with * have a significant difference from the control group ($p < 0.05$).	85
Figure 4.11	The ALP activity in hFOB 1.19 after 72 h treatment with Mg-BCP and BCP (mean \pm SD, n = 3). Data marked with * have a significant difference from the untreated group ($p < 0.05$).	87
Figure 4.12	The morphology of hFOB 1.19 (a) untreated cells and (b) after 72 h treatment with 50 $\mu\text{g}/\text{mL}$ Mg-BCP at 10x (first row), 20x (second row), and 40x (third row) magnifying powers.....	89
Figure 4.13	The morphology of hFOB 1.19 after 72 h treatment with (a) 200 $\mu\text{g}/\text{mL}$ and (b) 400 $\mu\text{g}/\text{mL}$ Mg-BCP at 10x (first row), 20x (second row), and 40x (third row) magnifying powers.....	90

LIST OF SYMBOLS AND UNITS

α	Alpha
α'	Alpha prime
\AA	Angstrom
\approx	Approximately equal to
atm %	Atom percent
β	Beta
cells/mL	Cells per milliliter
$^{\circ}$	Degree
$^{\circ}\text{C}$	Degree Celsius
2θ	Diffraction angle in XRD
F	Dilution factor
Eq	Equation
γ	Gamma
g	Gravitational force
h	Hour
$K\alpha$	K alpha emission line in XRD
kV	Kilovolt
$\mu\text{g/mL}$	Microgram per milliliter
μL	Microliter
mA	Milliampere
mg	Milligram
mg/mL	Milligram per milliliter
mL	Milliliter
mm	Millimeter
mmol/L	Millimole per liter

min	Minute
mol%	Mole percent
nm	Nanometer
n	Number of replicates
%	Percent
pH	Potential of hydrogen
P-value	Probability value
cm ⁻¹	Reciprocal centimeters
rpm	Revolutions per minute
R ²	Sum of the squares of the points' distances from the best-fit curve determined by nonlinear regression
v	Vibrational mode
λ	Wavelength
wt%	Weight percent

LIST OF ABBREVIATIONS

ACP	Amorphous calcium phosphate
ALP	Alkaline phosphatase
ANOVA	Analysis of variance
ATP	Adenosine triphosphate
BCA	Bicinchoninic acid
BSA	Bovine serum albumin
BCP	Biphasic calcium phosphate
Ca	Calcium
CaP	Calcium Phosphate
CDHA	Calcium deficient hydroxyapatite
Cl	Chloride
CoCr	Cobalt-chromium
Cu	Copper
DBPS/Modified	Dulbecco's phosphate-buffered saline without calcium and magnesium
DCPD	Dicalcium phosphate dihydrate (Brushite)
DMEM	Dulbecco's modified eagle medium
DMEM/F12	1:1 mixture of Dulbecco's modified Eagle medium and Ham's F-12 medium
DMSO	Dimethyl sulfoxide
d spacings	the Interplanar lattice spacings
ECM	Extracellular matrix
EDTA	Ethylenediamine tetraacetic acid
EDX	Dispersive X-ray analysis
F	Fluoride
FBS	Fetal bovine serum
Fe	Iron
FT-IR	Fourier-transform infrared spectroscopy
HA	Hydroxyapatite
hAT-MSC	Human adipose-derived mesenchymal stem cells
HBSS	Hank's balanced salt solution
HEPES	4-(2-hydroxyethyl)-1-piperazineethanesulfonic acid
hFOB 1.19	Human fetal osteoblasts

IC ₅₀	The half-maximal inhibitory concentration
ICDD	International center for diffraction data
IR	Infrared
J774	macrophage-like cell line
JCPDS	The joint committee on powder diffraction standards
K	Potassium
mag	Magnification scale
Mg	Magnesium
Mg-BCP	Magnesium-doped biphasic calcium phosphate
Mg-CDHA	Magnesium-doped calcium deficient hydroxyapatite
MSC	Mesenchymal stem cells
MTT	Thiazolyl blue tetrazolium bromide
Na	Sodium
NR	Neutral Red
O	Oxygen
OCP	Octa-calcium phosphate
OD	Optical density
P	Phosphorus
P ₂ O ₇ ⁻⁴	Pyrophosphate
Pb	Lead
PDF	Powder diffraction file
PGA	Polyglycolic acid
PLA	Polylactic acid
PO ₃ ⁻	Metaphosphate
PO ₄ ⁻³	Orthophosphate
PTH	Parathyroid hormone
SBF	Simulated body fluid
SCP-1	Human telomerase transcriptase transduced mesenchymal stem cells
SD	The standard deviation
SEM	Scanning electron microscope
Sr	Strontium
SV40	Simian virus 40
TCP	Tri Calcium Phosphate
Ti	Titanium

UV	Ultraviolet
XRD	X-ray diffractometer
Zn	Zinc

LIST OF APPENDICES

- APPENDIX A Certificates of Analysis and STR Report for hFOB 1.19 Cell Line.
- APPENDIX B Figure of the Optimization of Seeding Density, DMSO Volume, and Absorbance Wavelength for Cytotoxicity Assays at 24, 48, and 72 h, Respectively.
- APPENDIX C Table of Two-way ANOVA and Dunnett's Multiple Comparisons Test for Cell Viability after Treatment with Different Doses of Mg-BCP and BCP Powders Using MTT Assay. P-value < 0.05 Was Considered and Marked with*.
- APPENDIX D Table of Two-way ANOVA and Dunnett's Multiple Comparisons Test for Cell Viability after Treatment with Different Doses of Mg-BCP and BCP Powders Using NR Assay. P-value < 0.05 Was Considered and Marked with*.
- APPENDIX E The Standard Curve for (A) Phenol and (B) BSA in ALP Assay.
- APPENDIX F Table of Two-way ANOVA and Tukey's Multiple Comparisons Test for ALP Activity in Mature hFOB 1.19 after 72 h Treatment with Two Doses of Mg-BCP And BCP Powders and in Untreated Cells. P-value < 0.05 Was Considered.

**SINTESIS, PENCIRIAN, DAN KESITOTOKSIKAN SERBUK
MAGNESIUM-TERDOPAN KALSIUM FOSFAT (Mg-BCP) DWIFASA**

ABSTRAK

Baru-baru ini, pembedahan implan tulang dan gigi menjadi lazim dan kekurangan graf tulang semulajadi amat ketara. Oleh itu, keperluan graf tulang sintetik semakin meningkat. Kalsium fosfat sintetik (CaP) adalah biobahan yang boleh diserap dan bioserasi. CaP mempunyai komposisi kimia yang hampir sama dengan bahan mineral dalam enamel tulang dan gigi, terutamanya apabila CaP didopkan dengan ion yang berbeza. Oleh sebab ion magnesium (Mg) memainkan peranan yang penting dalam badan, Mg terdopan kalsium fosfat dwifasa (Mg-BCP) menarik perhatian para penyelidik berbanding dengan CaP lain-lain. Selain bioserasi, osteokonduktif, dan osteoinduktif, Mg-BCP mempunyai sifat mekanik yang lebih baik. Dalam projek ini, serbuk Mg-BCP dengan nisbah HA:TCP sama dengan 60:40 dan 1wt% Mg telah disintesis melalui kaedah pemendakan basah dan dicirikan dengan teknik XRD, SEM-EDX, dan FT-IR. Selepas itu, beberapa dos (1 hingga 400 $\mu\text{g}/\text{mL}$) serbuk Mg-BCP dikulturkan bersama sel hFOB 1.19 selama 24, 48, dan 72 jam untuk penilaian kesitotoksikan *in vitro* dan pemerhatian mikroskopik. Selain itu, aktiviti ALP dalam sel hFOB 1.19 diperiksa setelah 72 jam kultur dengan 50 dan 200 $\mu\text{g}/\text{mL}$ Mg-BCP. Untuk semua eksperimen, BCP dimasukkan untuk tujuan perbandingan. Serbuk Mg-BCP dengan nisbah komposisi fasa yang diinginkan (HA: β TCP = 60:40, 1wt% Mg) telah berjaya disintesis dan disahkan melalui analisis XRD, FT-IR, dan SEM-EDX. Eksperimen kesitotoksikan menunjukkan bahawa serbuk Mg-BCP mengurangkan kebolehhidupan sel hFOB 1.19. Walau bagaimanapun, pengurangan kebolehhidupan tersebut tidak teruk walaupun sel

hFOB 1.19 tersebut dikultur dengan dos serbuk Mg-BCP yang tertinggi (400 µg/mL) untuk tempoh inkubasi terpanjang (72 jam); peratus kebolehidupan sel hFOB 1.19 adalah lebih daripada 83% tanpa perubahan pada morfologi sel. Yang menariknya, serbuk Mg-BCP kurang toksik daripada BCP. Tambahan pula, peningkatan dos Mg-BCP juga meningkatkan aktiviti ALP dalam sel hFOB 1.19 dengan ketara berbanding dengan serbuk BCP. Kesimpulannya, serbuk Mg-BCP dengan nisbah komposisi fasa HA:βTCP = 60:40 dan 1 wt% Mg adalah pengganti graf tulang sintetik yang berpotensi.

**SYNTHESIS, CHARACTERIZATION AND CYTOTOXICITY
EVALUATION OF MAGNESIUM-DOPED BIPHASIC CALCIUM
PHOSPHATE (Mg-BCP) POWDERS**

ABSTRACT

Recently, bone and dental surgeries are becoming remarkably prevalent, and the natural bone grafts shortage in this area is evident. Thus, the need for synthetic bone graft substitutes is increasing. Synthetic calcium phosphates (CaPs) are ideal, resorbable, and biocompatible biomaterials that are almost identical to the mineral part of the bone and tooth enamel, especially when they are doped with different ions. Since magnesium ion (Mg) performs significant functions throughout the human body, Mg-doped biphasic calcium phosphate (Mg-BCP) gets special attention among other CaPs. Besides biocompatibility, osteoconductive, and osteoinductive properties, Mg-BCP has better mechanical properties. In this project, Mg-BCP powder with HA:βTCP ratio equals 60:40, and Mg substitution of 1 wt% was synthesized using the chemical wet precipitation method and characterized via XRD, SEM-EDX, and FT-IR techniques. After that, several doses (1 to 400 μg/mL) of Mg-BCP were co-cultured with hFOB 1.19 cells for 24, 48, and 72 h for *in vitro* cytotoxicity evaluation and microscopic observation. Additionally, alkaline phosphatase (ALP) activity of hFOB 1.19 cells was investigated after 72 h co-culture with 50 and 200 μg/mL doses of Mg-BCP. For all the experiments, pristine BCP was included for comparison purposes. As a result, Mg-BCP powder with the desired phase composition ratio (HA:βTCP = 60:40, 1 wt% Mg) was successfully synthesized as confirmed by XRD, FT-IR, and SEM-EDX analysis. Cytotoxicity evaluation indicated that Mg-BCP did cause a certain reduction in cell viability.

However, the reduction was not severe even when hFOB 1.19 cells were co-cultured with the highest dose of the synthesized powder (400 μ g/mL) for the longest incubation period (72 h); the cell viability was above 83% with no changes in the cell morphology. Interestingly, the Mg-BCP powder was less toxic than BCP. Moreover, increasing the Mg-BCP dose significantly enhanced the ALP activity in hFOB 1.19 cells compared to BCP and untreated cells. In conclusion, the Mg-BCP powder with a phase composition ratio equals 60:40 and 1 wt% Mg is a promising bone graft substitute.

CHAPTER 1

INTRODUCTION

1.1 History of Bone Substitutes

Bone is a dynamic tissue with regenerative characteristics. Normally, this tissue is able to repair its small defects effectively. However, this process fails in significant defects. Therefore, bridging materials are needed to support bone healing and, if possible, stimulate its growth (Ginebra et al., 2018). Orthopedic implants were initially a list of unsuccessful failed attempts with plenty of rejection, metal toxicity, and sepsis instances. In 1892, calcium sulfate succeeded as the first synthetic ceramic used to fill bone defects in tuberculosis infection (Hollinger et al., 1996). Calcium sulfate was later applied to repair huge bone damages and reconstruct craniofacial bones during the Vietnam War (Kelly, 1973).

The initially published studies on bone autografts and allografts date back to the 19th century, specifically when a German surgeon and ophthalmologist successfully applied bone autograft to replace parts of the skull (Eliaz & Metoki, 2017). A successful application of allografts was achieved sixty years later; a Scottish surgeon used a bone allograft generated from the tibia of a child with rickets to rebuild an infected humerus of a 4-year-old boy (Eliaz & Metoki, 2017). After that, artificial calcium phosphates (CaP) were used for the first time as a powder form; it was mixed with lactic acid and put on an open pulp tissue. The history of CaP bioceramic implants started in 1920 when an American surgeon surgically created fractures in a rabbit bone and then injected triple calcium phosphate (TCP) implant into the resulted fractured gaps. TCP induced bone growth and union compared to the controls (Albee, 1920; Eliaz & Metoki, 2017; Ginebra et al., 2018). Regarding humans, the first applied implant was intended for a dental defect in 1965.

This was followed by the earliest orthopedic use of hydroxyapatite (HA) in humans as a coating for a hip prosthesis with a thickness of 200 μm in 1985. However, the use of CaPs as bone scaffolds has not been accomplished until 1994 (Eliaz & Metoki, 2017). Since then, the applications of CaPs bioceramics were expanded, covering all areas of the skeleton due to their chemical similarity to the natural bone, including spinal fusion, craniomaxillofacial reconstruction, treatment of bone defects, fracture treatment, total joint replacement (bone augmentation), and revision surgery (Best et al., 2008; Hench, 1991).

1.2 Calcium Phosphate Bioceramics as Bone Substitutes

The first and most important criterion for a biomaterial to be applied as a bone substitute is to be biocompatible. Biocompatibility indicates the ability of the biomaterials to be implanted into the body and perform their intended function without triggering any adverse local or systemic host response (Cohn et al., 2017; Heimann, 2002). Other essential characteristics of biomaterials include osteoinductivity and/or osteoconductivity. Osteoinductive materials induce the maturation of osteoblasts during the bone healing process and prompt the osteogenesis process, which is the natural process to form a new bone. On the other hand, osteoconductive materials do not accelerate osteogenesis; however, they permit bone growth on their surfaces (Daculsi et al., 2013; Heimann, 2002).

CaPs are the first ideal, resorbable, and biocompatible bone graft substitutes (Bohner et al., 2012). CaPs are a group of minerals mainly composed of calcium (Ca) cations and phosphate anions, including orthophosphate (PO_4^{-3}), metaphosphate (PO_3^-), and pyrophosphate ($\text{P}_2\text{O}_7^{-4}$). They receive a specific focus because they are almost identical to the mineral part of the bone and tooth enamel and have excellent

potential in biomaterials research (Ginebra et al., 2018). The most common CaPs in use are HA, α - and β TCP, octa-calcium phosphate (OCP), amorphous calcium phosphate (ACP), and biphasic calcium phosphates (BCP). In addition to their similarities to the biologic precursors of bone mineral, these synthetic CaPs have osteoconductive properties because of their high affinity for protein adsorption and growth factors (Ebrahimi et al., 2017).

HA is a significant ingredient of natural bone. As an implant, it has osteoconductive characteristics. It is proven to bond mechanically and chemically with the bone tissues until they gradually replace HA in the implanted ceramic (Gao et al., 2014; Tracy & Doremus, 1984). However, HA has poor biodegradation, osteoinductivity, and bio-solubility properties (Chang et al., 2000; Webler et al., 2015).

On the other hand, TCP outperforms HA in terms of solubility, osteoinductivity, and biodegradability (Gao et al., 2014; Webler et al., 2015). There are four polymorphs of TCP; α , α' , β , and γ . The latter can be formed by heating the β phase to 950°C under high pressure of 4.0 GPa. The stability of these four polymorphs differs from one phase to another. β TCP is the stable phase beneath 1125°C, α phase is stable between 1125°C and 1430°C, whereas α' phase is stable above 1430°C. Noticeably, the phases α' and γ are the hardest to produce as they require high temperature and high pressure during the synthesis process, respectively. α TCP high reactivity results in high degradability. Thus, it is undesirable for bone substitution. Consequently, β TCP is the preferable polymorph because of its moderate and desirable degradability, in addition to its stability in normal conditions. Therefore, the β TCP is always under the spotlight gaining much more attention from the researchers as compared to its derivatives (Mathew &

Takagi, 2001; Ryu et al., 2004).

In fact, the solubility of a biomaterial is an important factor in controlling its bioactivity. This inspired researchers to combine HA and β TCP and form a biphasic mixture called BCP. BCP is a bioceramic mixture consists of the poorly soluble HA (chemical formula: $\text{Ca}_5\text{O}_{12}\text{P}_3(\text{OH})$, with a Ca to phosphorus (P) (Ca/P) ratio of 1.67) and the soluble β TCP (chemical formula: $\text{Ca}_3\text{O}_8\text{P}_2$, with a Ca/P ratio of 1.5). This combination offers significant advantages over single-phase CaPs since the stable HA functions as a scaffold that provides a structural framework for the newly formed bone. Additionally, the biodegradation of β TCP creates space for the new bone ingrowth and oversaturates the local environment with Ca^{+2} ions during the biodegradation process to accelerate the new bone formation (Frayssinet et al., 1993; Kohri et al., 1993; Webler et al., 2015). In short, the β TCP compensates for the poor biodegradation properties of HA and stimulated bone growth without altering the osteoconductive characteristics of HA (Ryu et al., 2004; Wang et al., 1998; Webler et al., 2015). Moreover, researchers have gone further and controlled the solubility of the BCP by adjusting the ratio of HA: β TCP. Studies indicate that the optimum ratio of HA: β TCP is in the range between 70:30 and 60:40 (Frayssinet et al., 1993; Kohri et al., 1993; Webler et al., 2015). This distinguishing feature favored the use of BCP for bone reconstruction (Bouler et al., 2017).

1.3 Magnesium Doped Biphasic Calcium Phosphate: A Better Bone

Substitute

Natural bone is composed of 60 – 70% inorganic CaPs, mainly, nonstoichiometric HA substituted with several ions, including sodium (Na^+), potassium (K^+), magnesium (Mg^{+2}), zinc (Zn^{+2}), iron (Fe^{+2}), copper (Cu^{+2}), strontium

(Sr^{+2}), lead (Pb^{+2}), citrate ($\text{C}_6\text{H}_5\text{O}_7^{-3}$), hydrogenphosphate (HPO_4^{-2}), carbonate (CO_3^{-2}), chloride (Cl), fluoride (F) (Eliaz & Metoki, 2017). Among all these ions, studies on metal Mg ions are particularly interesting. First, Mg is the fourth prevalent cation in the human body, and the second spread intracellular cation. In the human body, 65% of this lightest metal is kept in teeth and cortical bone matrix. Second, Mg plays multiple important roles in the human body, such as controlling the sodium and calcium ion channels, stabilizing genetic materials, acting as catalyzer and cofactor enzymes, as well as playing a major role in bone growth (Ballouze et al., 2021). Lack of Mg in the human body is found to decrease the bone cells' activity, which then leads to reduced bone growth, increased bone fracture risk because of low bone mass, and osteoporosis.

For that, Mg addition to BCP not only provides high similarity to the inorganic portion of the natural bone, it might also promote the osteogenesis and healing processes and consequently increases its suitability for clinical applications (Gomes et al., 2009; Kim et al., 2013).

Furthermore, Mg addition also enhances the physicochemical properties of BCP. First, the Mg insertion in BCP increases the thermal stability of β TCP and delays its conversion to α TCP until 1400°C (Gomes et al., 2009). This feature is of high importance during the sintering process when BCP is exposed to high temperatures in order to produce porous materials or granules for orthopedic applications in bone augmentation surgeries and bone grafting (Ballouze et al., 2021; Kannan et al., 2009; Kumar et al., 2015; Ryu et al., 2004). Second, the ratio of HA and β TCP in BCP can be modulated through Mg incorporation. Mg insertion will reduce the thermal stability of HA leading to its transformation into β TCP (Aina et al., 2012; Chaudhry et al., 2008). Mg supports the formation of β TCP over the HA

regardless of the BCP synthesis route (Dickens et al., 1974; Gomes et al., 2009; Kannan et al., 2009; Sopyan et al., 2011; Toibah et al., 2008). Thus, the ratio of HA and β TCP in BCP could be adjusted by Mg insertion. Besides that, Mg also improves the BCP's density and mechanical strength (Marahat et al., 2020). Thus, this feature enables magnesium-doped biphasic calcium phosphate (Mg-BCP) scaffolds to overcome the brittleness and the weak mechanical strength of CaPs scaffolds, particularly when implanted into a load-bearing site (Kannan et al., 2005; Sopyan et al., 2011; Sopyan & Rahim, 2012). The better physicochemical properties of Mg-BCP compared to other CaPs makes it a good candidate as a synthetic bone substitute. However, so far, only limited investigations have been carried out.

1.4 Problem statement

Mg-BCP powders are intended to be used as bone substitutes in bone and dental surgeries where the biological environment surrounding the implantation site will be exposed to high concentrations of the biomaterial. However, *in vitro* data available in the published articles were not adequate, and none of these reports investigated the biocompatibility of Mg-BCP on human osteoblast. Since osteoblast is one of the main key players in the osteogenesis process and the cells will directly interact with the biomaterials, the potential safety and risk of the Mg-BPC on the osteoblasts should be addressed clearly. Moreover, the Mg-BCP concentrations that were applied in previous reports were low (0.001 – 1 μ g/mL) (Kannan et al., 2009) and did not reflect the real situation of the implant site. In reality, the bone cells will interact with more than 1 μ g/mL of Mg-BCP on the implant site. Thus, it is appropriate to carry out more *in vitro* biocompatibility tests using higher concentrations of the synthesized powders and human osteoblasts. In this project, the

biocompatibility of the synthesized Mg-BCP on human fetal osteoblast (hFOB 1.19) was evaluated. Furthermore, the effect of Mg-BCP on the osteoblasts' differentiation and the osteogenesis properties was tested by measuring the alkaline phosphatase (ALP) activity in hFOB 1.19 cells. This is of great importance in order to estimate Mg-BCP osteoconductive properties.

1.5 Objectives of the study

The main objective of the study is to synthesize Mg-BCP powder and determine its biocompatibility and its osteogenesis effect on human fetal osteoblasts cell line hFOB1.19.

The sub-objectives of this study are:

1. To synthesize and characterize the physicochemical properties of the Mg-BCP powders,
2. To evaluate the cytotoxic effects of the synthesized Mg-BCP powder on hFOB1.19, and
3. To determine the effect of the Mg-BCP powder on the ALP enzymatic activity level of hFOB1.19 cells.

CHAPTER 2

LITERATURE REVIEW

2.1 Bone Tissue and the Bone Repair Process

Bone is a dynamic tissue that is consisted of cells implanted in an extracellular matrix (ECM). The ECM is composed of 10 – 20% organic phase, which is mainly a network of fibrous proteins and collagen fibers, 60 – 70% inorganic phase consists of inorganic CaPs (mainly in the form of HA), and 9 – 20% water (Brannigan & Griffin, 2016; Fattore et al., 2012; Kalfas, 2001; Wegst et al., 2015). The composition of bone minerals also contains other ions, such as Na^+ , K^+ , Mg^{+2} , Zn^{+2} , Fe^{+2} , Cu^{+2} , Sr^{+2} , Pb^{+2} , HPO_4^{-2} , CO_3^{-2} , Cl^- , and F^- . On the other hand, the organic component of bone is composed of type I collagen and a small amount of non-collagenous proteins (glycoproteins, growth factors, and proteoglycans). Aside from mineral and protein components, bone is also populated by cells and blood vessels. They include osteoprogenitor cells, osteoblasts, osteocytes, bone lining cells, and osteoclasts. These cells are involved in maintaining a healthy bone structure.

Bone has three essential types of cells. Osteocytes are originated from mature osteoblasts and count over 90% of the total count of bone cells; they are located in the bone matrix as mechano-sensors to organize the bone remodeling. The second type of bone cell is the osteoclasts; they are large multinucleated cells originating from the monocyte-macrophage line, and their function is bone resorption (Fattore et al., 2012). The third type is osteoblasts; they are originated from the mesenchymal stem cells (MSC) and are responsible for the osteogenesis process (Fattore et al., 2012). Osteoblasts secrete ECM proteins forming the unmineralized bone matrix or osteoid that subsequently become templates onto which the inorganic minerals are deposited and undergo mineralization. The ECM proteins assist in the construction of

the osteoid. Osteoblasts also secrete ALP enzyme to degrade the phosphate-containing compounds releasing phosphate ions inside the osteoid. After that, the mineralization process for the bone matrix starts when osteoblasts utilize the free Ca and phosphate ions to form HA, which takes its place between the collagen fibers (Fattore et al., 2012; Kannan et al., 2009).

The bone healing process can be direct or indirect. Direct healing takes place when the injured bone surfaces are still tightly stabilized close to each other. This happens typically in flat bones, such as the skull. In this case, the osteoblasts originate from MSC to start the ossification process. The other indirect process happens to cover a bigger gap between the injured bone surfaces. It typically occurs in long bones. The indirect process involves an initial cartilage formation called the "soft callus" followed by the ossification process by the osteoblasts (Bahney et al., 2019). When a bone injury occurs, the impaired bone structure and vascular supply disrupt the mechanical stability and the tissue oxygenation and nutrition. At the same time, a blood clot forms to preserve homeostasis as a temporary scaffold and release cytokines to attract the inflammatory cells. These inflammatory cells first excrete inflammatory cytokines that cause a generalized acute inflammatory response and then release multiple growth factors that in turn promote the proliferation and differentiation of the stem cells to start the repair process (Bahney et al., 2019; Schell et al., 2017). After the inflammation phase, the angio-mesenchymal phase starts. During this phase, the revascularization of the callus takes place by the angiogenesis (the existing vasculature forms new blood vessels) and the neovascularization (de novo composing of new blood vessels) processes. Another important aspect of this phase is the differentiation of the MSCs into osteoblasts and chondrocytes in order to start the direct or indirect bone formation phase (Bahney et al., 2019; Ghiasi et al.,

2017; Locke et al., 2011). The direct phase involves MSCs differentiation into osteoblasts that create the bone tissue. On the other hand, in the indirect phase, the MSCs differentiate into chondrocytes that synthesize the cartilage tissue and go through apoptosis. After that, the remodeling process starts when the osteoblasts synthesize the hard bone tissue to replace the cartilage with the help of the osteoclasts. The osteoclasts perform the degradation process of the soft bone and stimulate the bone osteogenesis until finally they also conclude with apoptosis (Bahney et al., 2019).

2.2 Bone Grafting Materials

Bone is the second tissue in the body that is most subjected to transplantation after blood transfusion (Ehrler & Vaccaro, 2000; Elsalanty & Genecov, 2009; Oryan et al., 2014). Besides accidents, plenty of skeleton defects are observed due to the increased aging population in addition to the several diseases that affect the bone and joints, such as osteoporosis, arthritis, obesity, diabetes, and cancer (Xia et al., 2017). Statistical data refers that annual bone grafting surgeries count up to approximately 2.2 million procedures per year, not to forget the need for dental implants has risen to 10000 – 30000 a year (Basu & Basu, 2019b). The demand for bone grafting materials and the number of procedures requiring these products will continue to increase as the population ages and the physical activity of the elderly population increases.

A bone graft is an implanted substance that enhances bone recovery and reformation; it can be used as a single material or along with additional element (s) (Elsalanty & Genecov, 2009; Oryan et al., 2014). Basically, the bone graft substitutes should have three essential standards. They should be; resorbable to avoid fatigue

fractures due to long implantation periods, osteoinductive to allow the bone tissue to grow on their surfaces, and have excellent mechanical strength, same as the cortical bone (Bohner et al., 2012). Bone grafts can be classified into two main categories, natural grafts that include autografts, allografts, and xenografts, while synthetic biomaterials include metals, polymers, and bioceramics. Combinations of synthetic biomaterials are also common (Dimitriou et al., 2011; Oryan et al., 2014). In minor defects, the autografts stand as the ideal grafts since they are obtained from another location in the same individual. Therefore, they offer osteogenic cells, osteoinductive growth factors, and osteoconductive scaffolds. They are either cancellous or cortical or a combination of both (Athanasίου et al., 2010; Oryan et al., 2014). However, autografts can induce soreness and morbidity at the location of donation in addition to the vascular damages throughout the harvesting process (Ehrler & Vaccaro, 2000; Oryan et al., 2014). Other natural grafts in use are allografts; they are harvested from another individual of the same species. Although they have the osteoinduction and osteoconduction properties of autografts, they are higher in cost with a rejection risk, site infections possibility, and deficiency of the osteogenic characteristics (Dimitriou et al., 2011; Oryan et al., 2014). The less desirable natural grafts are xenografts because they are obtained from an individual of another species. They have the same pros and cons of allografts in addition to the risks of transmission of zoonotic diseases and the higher rejection possibility (Oryan et al., 2013, 2014).

On the other hand, the synthetic biomaterials include three main categories; metals (such as stainless steel, cobalt-chromium (CoCr), and Titanium (Ti) alloys), polymers (natural polymers such as collagen type I and synthetic polymers such as polylactic acid (PLA) and polyglycolic acid (PGA)), and ceramics (CaPs ceramics such as HA and TCP) (Amin & Ewais, 2017; Oryan et al., 2014; Prasad et al., 2017).

Ceramics may be bioinert (e.g., alumina and zirconia), resorbable (e.g., TCP), or bioactive (e.g., HA, bioactive glasses, and glass-ceramics) (Hench, 1991). Bioceramics are synthetic biomaterials used to repair and reconstruct the diseased or damaged parts of the musculoskeletal system. They are associated with the best tissue responses and the most effective bonding to the bone, whereas natural polymer-based scaffolds are highly bioactive and biodegradable. But they both lack the good mechanical characteristics of metals. Consequently, bioactive ceramic combinations with metal elements are very promising potential approaches with remarkable results (Amin & Ewais, 2017; Baino et al., 2015). For example, the addition of Mg to CaPs controls their stability and mechanical strength.

2.3 Calcium Phosphates

Among all synthetic bone graft materials, CaPs receive a specific focus because they are almost identical to the mineral part of the bone (Ginebra et al., 2018). Besides, they have a high affinity for protein adsorption and growth factors (Bohner et al., 2012; Ebrahimi et al., 2017). Therefore, CaPs are biocompatible cements that do not trigger any inflammatory biological response (Eliaz & Metoki, 2017). CaPs are also considered ideal, resorbable, osteoconductive, and osteoinductive bone graft substitutes (Bohner et al., 2012; Ebrahimi et al., 2017). Osteoinductive CaPs are able to enhance the differentiation of progenitor cells toward the osteoblasts and consequently promote the osteogenesis process. Osteoconductive CaPs can support the proliferation of mature osteoblasts and allow the formation of bone directly on the cements' surfaces (Lobo & Arinzeh, 2010). At the implantation site, CaPs should undergo a partial dissolution releasing their ionic constituents and gradually increasing the Ca and phosphate concentrations in the

surrounding environment. These ions are then recomposed by the bone osteoblasts into biologic HA that precipitate on the implant's surface (Eliaz & Metoki, 2017). The partial and gradual dissolution of CaPs is requested in order to achieve their bioactivity and avoid their complete dissolution before the construction of the bone is completed (Lobo & Arinzeh, 2010).

The biological behavior, in other words, the cell-biomaterial interaction begins with an interaction between the material surface and the water molecules that creates a hydration shell. This is followed by an interaction between the proteins that existed in the surrounding water layer with the newly formed hydration shell around the surface of the biomaterial. The result of this process is the adsorption of the proteins on the CaPs surface. Finally, the latter adsorbed proteins interact and attach to the proteins of the bone cell surface receptors and as a conclusion, the cells adhere to the surface of the biomaterial (Basu & Basu, 2019b). Many factors control the protein adsorption and the cell adhesion on the surface of CaPs such as the particle size, the surface charge, pH, the solubility of the biomaterial, the ionic composition, the electrostatic forces, etc. Higher protein adsorption was associated with the smaller particle size (preferably less than 100 nm). Another important factor that favors the protein adsorption mechanism and consequently the cell adhesion is the electrostatic interactions between the positively charged ions (cations) on the CaPs surface (such as Ca) and the negatively charged oxygen (O) atoms of the carboxyl groups in the amino acids and in the small peptide chains. An additional factor is the hydrogen bonds between the H atoms in the amino acids and the O atoms of the phosphate groups in CaPs (Basu & Basu, 2019b). The previously stated interactions between the CaP surface and the proteins and other biological molecules differ in

their nature and intensity and directly affect the cytocompatibility and osteogenesis properties of the biomaterial (Basu & Basu, 2019b).

The most common CaPs in use are HA, α and β TCP, OCP, ACP, and BCP. Multiple forms of these CaPs have been applied, including pastes, cements, coatings, and scaffolds (Eliaz & Metoki, 2017). HA was first named by a German geologist in 1786 after the ancient Greek term "apatao", which means "to mislead". It exists in either a monoclinic or a hexagonal phase. Although the chemical formula of HA is $\text{Ca}_5(\text{PO}_4)_3(\text{OH})$, it is usually expressed as $\text{Ca}_{10}(\text{PO}_4)_6(\text{OH})_2$ to refer that its hexagonal unit cell typically contains two HA molecules. This hexagonal structure is found in natural bone and is commonly involved in biological and medical applications (Basu & Basu, 2019b; Eliaz & Metoki, 2017). The synthesized HA has been used for various clinical applications between bone repair and augmentation surgeries, implants coatings, drug delivery, and toothpaste (Eliaz & Metoki, 2017). In term of stability as compared to other CaPs, HA is ordered after fluorapatite as the second most stable CaP, thus, the second least soluble CaPs (Chang et al., 2000; Eliaz & Metoki, 2017; Webler et al., 2015). Despite its poor solubility, HA is biocompatible and osteoconductive (Eliaz & Metoki, 2017). It enhances the precipitation of the newly formed apatite crystals on its surface. Moreover, it can mechanically and chemically form bonds with the host bone tissues until the newly formed bone gradually replaces HA in the implant site (Eliaz & Metoki, 2017; Gao et al., 2014; Tracy & Doremus, 1984). However, HA is reported to have several drawbacks regarding its poor biodegradation, low solubility, high fragility, and the lack of osteoinductive properties (Chang et al., 2000; Eliaz & Metoki, 2017; Webler et al., 2015).

TCP was first introduced in 1832 with the name of "tribasic phosphate of lime", and later, it took its current name after its chemical composition $\text{Ca}_3(\text{PO}_4)_2$, which has a Ca/P ratio equals 1.5 (Eliaz & Metoki, 2017). There are four polymorphs of TCP: β , α , α' and, γ . As presented in the phase diagram of HA and TCP (Figure 2.1), the γ TCP can be formed by heating the β phase to 950°C in addition to the high pressure of 4.0 GPa. α' phase is obtainable and stable only at a temperature above 1430°C. Obviously, α' and γ phases are not preferred for bone grafting since they are not stable in normal conditions (Mathew & Takagi, 2001; Ryu et al., 2004). α TCP is mainly prepared by heating β TCP to a temperature above 1125°C. Although the chemical composition of α and β TCP is the same, yet their solubility, stability, and crystal structure are different. The α polymorph is less stable and has higher reactivity and resorption rate. Its high resorption rate exceeds the rate of the new bone formation, thus, restrict its usage in biomedical applications (Eliaz & Metoki, 2017). Consequently, the β TCP polymorph is the best choice for biomedical applications (Eliaz & Metoki, 2017; Mathew & Takagi, 2001; Ryu et al., 2004). The β TCP cell unit involves 21 units of $\text{Ca}_3(\text{PO}_4)_2$ units. The β TCP is reported to be a biocompatible substance with osteoinductive and osteoconductive properties; furthermore, it supports apatite formation on its surface (Eliaz & Metoki, 2017; Gao et al., 2014). It was used as bone cement, a biomaterial in dentistry, a polishing agent in toothpaste, and a food supplement called E341. β TCP based products, namely, Bio-Lu Bioceramics (China), calc-i-oss classicTM (Switzerland), SynthoGraftTM (U.S.), OSferionTM Trapezoid (U.S.), Biosorb® (France), Cerasorb® Dental M (U.S.), VitossTM Bone Graft Substitute (U.S.), and chronOSTM (U.S.) have been commercialized (Eliaz & Metoki, 2017; Mathew & Takagi, 2001).

The Phase Diagram of HA and TCP

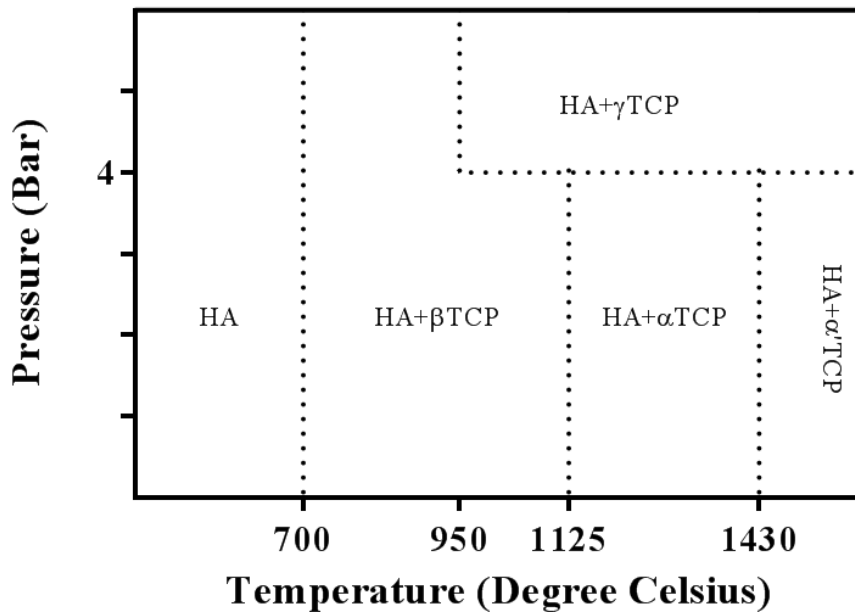


Figure 2.1 The phase diagram of HA and TCP.

In fact, the solubility of CaPs is probably one of their most important chemical properties since it controls their bioactivity and interferes with the osteogenesis process. This was the first motive to create a biphasic mixture of HA and β TCP. This mixture has been called BCP since 1986. It combines the poorly soluble and osteoconductive HA with the more soluble osteoinductive β TCP creating a good balance between stability and solubility of CaPs (Eliaz & Metoki, 2017; Ryu et al., 2004; Wang et al., 1998). By adjusting the ratio of HA: β TCP in the biphasic mixture, the solubility, osteoinductivity, and osteoconductivity of the BCP can be controlled. This distinguishing feature favored BCP use over other biomaterials for clinical applications (Basu & Basu, 2019b; Bouler et al., 2017). BCP offers significant advantages over single-phase CaPs; the stable HA phase functions as a scaffold and provides a structural framework for the newly formed bone. At the same time, the biodegradation of β TCP creates space for new bone ingrowth and oversaturates the local environment with Ca and phosphate ions to promote the new

bone formation. It is reported that the optimum phase composition ratio of HA: β TCP is in the range between 70:30 and 60:40 (Frayssinet et al., 1993; Kohri et al., 1993; Webler et al., 2015), although only the ratio of 60:40 has been successfully engaged in clinical trials so far (Danesh-Sani et al., 2016; De Oliveira Lomelino et al., 2012; Rodríguez et al., 2007).

However, a serious drawback that restricts the CaPs clinical applications is their poor mechanical strength. In fact, some load-bearing sites, such as the hip joint, are subjected to a load of three times of the body weight, and this load becomes enormous when performing some activities such as jumping where the load can reach 10 times the body weight (Eliaz & Metoki, 2017). Unfortunately, CaPs are still relatively brittle to afford all this load-bearing because of their porosity. Consequently, most of the CaPs are usually used as implants in non-load bearing sites, fillers for bone defects, and coatings for other metallic implants (Eliaz & Metoki, 2017). To overcome this weakness of CaPs, several attempts have been performed by researchers, including inserting Mg into the BCP, which proved to significantly improve its mechanical strength (Marahat et al., 2020).

2.4 Mg-doping of CaPs towards Developing Mg-BCP

Many attempts have been performed to incorporate ions in the HA and β TCP lattice structure to further improve their bioactivity, biocompatibility, and mechanical strength (Ballouze et al., 2021). Furthermore, in order to mimic the chemical composition of the natural bone, doping CaP based biomaterials with the ions found in natural bones (Table 2.1) can definitely favor the process of osteogenesis and rapid healing (Habibovic & Barralet, 2011). Among these ions, Mg has sorted the fourth spread cation in the human body (Gomes et al., 2009) and the second most

prevalent intracellular cation (Nabiyouni et al., 2018). Interestingly, 60% of the total body Mg is stored in bone and found in the hydration shell around the biologic apatites or attached to their surface (Laskus & Kolmas, 2017).

Table 2.1 The weight percentage (wt%) composition of inorganic phases of adult human calcified tissues (Kannan et al., 2008).

Composition (wt%)	Enamel	Dentin	Bone
Calcium	36.5	35.1	34.8
Phosphorus	17.7	16.9	15.2
Ca/P (molar ratio)	1.63	1.61	1.71
Sodium	0.50	0.60	0.9
Magnesium	0.44	1.23	0.72
Potassium	0.08	0.05	0.03
Carbonate (as CO ₃ ⁻²)*	3.5	5.6	7.4
Fluoride	0.01	0.06	0.03
Chloride	0.30	0.01	0.13

* Note that the content of CO₃⁻² is indicated as an un-ashed sample, whereas the other elements are indicated as analyzed in ashed samples.

Generally, Mg performs significant functions throughout the human body. These functions involve controlling the Ca and Na ion channels, stabilizing the cellular DNA, being a cofactor and catalyzer for many enzymes, and enhancing cell growth and proliferation (Nabiyouni et al., 2018). In addition to its previous vital roles, Mg has specific functions in preserving the balance of the mineralized tissues in either a direct or an indirect way. Regarding its indirect influence, Mg interferes with the secretion of the parathyroid hormone (PTH) and subsequently the vitamin D synthesis in the kidney. Mg deficiency is reported to cause a drop in the serum concentrations of PTH and vitamin D and consequently result in hypocalcemia (Laskus & Kolmas, 2017). The direct influence, on the other hand, has two main aspects. First, Mg influences the crystal structure of bone; its low levels are associated with hypomagnesemia. In this case, the bone tries to recover by recruiting

its ionic deposits, which in turn causes some defects to the structure of its biologic apatite and decreases the bone mechanical strength (Laskus & Kolmas, 2017). The second aspect of the Mg's direct effect on the mineralized tissues is the influence of Mg on the bone cells' activity. This is confirmed by both *in vitro* and *in vivo* investigations (Laskus & Kolmas, 2017). *In vitro* studies on bone cell cultures indicated that the presence of Mg stimulates osteoblast proliferation, adhesion, and growth during the early stage of osteogenesis (Laskus & Kolmas, 2017; Nabiyouni et al., 2018; Sopyan et al., 2011; Sopyan & Rahim, 2012). Moreover, the proliferation rate, differentiation, and mineralization of preosteoblast cultures were stimulated by the presence of Mg and Ca ions in the culture medium (Nabiyouni et al., 2015). Low and medium Mg concentrations increased the mineralization of the ECM and enhanced the collagen and other proteins expression (Nabiyouni et al., 2018). On the other hand, the deficiency of Mg is associated with inflammatory disorders. The inflammation status results in osteoclasts induction and osteoblasts activity reduction in bone, leading to bone fragility, low bone mass, reduced bone growth, and osteoporosis (Castiglioni et al., 2013; Laskus & Kolmas, 2017; Nabiyouni et al., 2018).

From the physiochemical perspective, the addition of Mg to CaP controls their stability, solubility, and mechanical strength. Mg doping in HA increases its solubility and degradability in the biological fluids (Alshemary et al., 2015; Batra et al., 2013; Chaudhry et al., 2008; Kolmas et al., 2011). It also improves its osteoconductive properties (Xia et al., 2017). Regarding β TCP, Mg is undoubtedly the most substituted dopant in its lattice because it stabilizes the β TCP phase and improves its mechanical strength (Laskus & Kolmas, 2017). Moreover, the Mg doping decreases the initial sintering temperature and increases the resulted particle

size of Mg-doped β TCP (Babaie et al., 2016; Ballouze et al., 2021; Nabiyouni et al., 2018). Besides the aforementioned physicochemical characteristics, *in vitro* studies reported an improvement in the osteoconductive properties of Mg-doped β TCP (Ballouze et al., 2021).

Since Mg substitution in HA and β TCP provided several advantages, a mixture of HA and β TCP doped with Mg has gained significant attention recently. Figure 2.2 presents the crystal structure of HA and β TCP (Ballouze et al., 2021; Kannan et al., 2008). Studies found that the Mg ions preferred to accommodate and replace Ca ions of the β TCP lattice instead of the HA. Mg substitutes the Ca ions in the β TCP phase because the cation sites are smaller than that of HA; therefore, the small Mg ion can fit better into it. Moreover, there is a short distance between a specific Ca ion in the β TCP lattice and the adjacent O ion, causing a high electrostatic repulsion at this site. This repulsion decreases when the Mg ion occupies this Ca site because of its smaller radii (Ballouze et al., 2021; Kumar et al., 2015). Besides that, studies also found that the HA and β TCP ratio in BCP can be controlled by the Mg addition. Since Mg is engaged within the β TCP lattice in BCP, it supports the formation of this phase over the HA phase regardless of the applied synthesis route. Thus, the proportion of β TCP increases with the increase in Mg substitution in BCP (Dickens et al., 1974; Gomes et al., 2009; Kannan et al., 2009; Sopyan et al., 2011; Toibah et al., 2008).

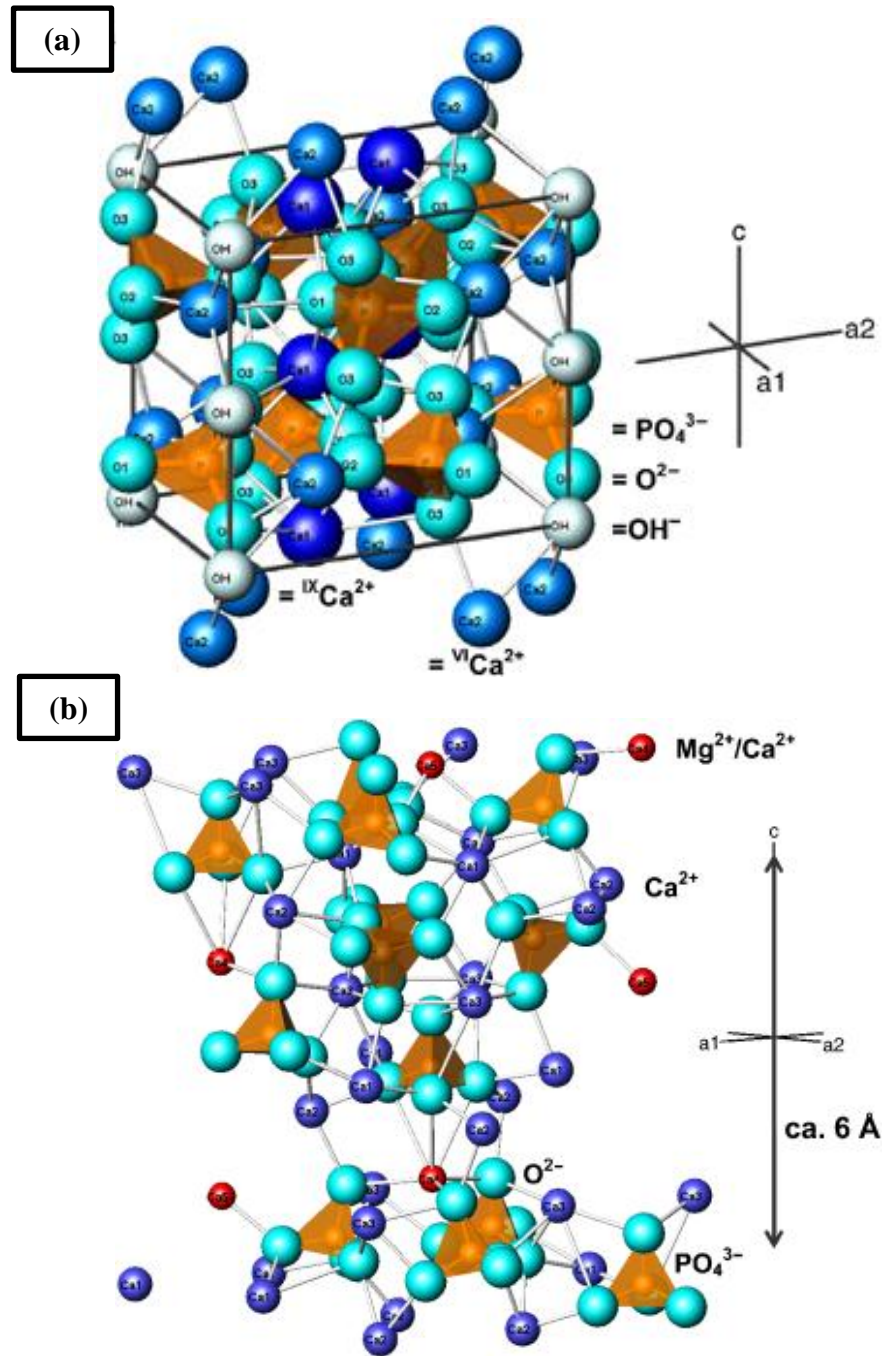


Figure 2.2 The crystal structure of (a) HA and (b) β TCP where Mg preferentially accommodates in the Ca(4) and Ca(5) site (red in color) of the β TCP lattice (Ballouze et al., 2021; Kannan et al., 2008).

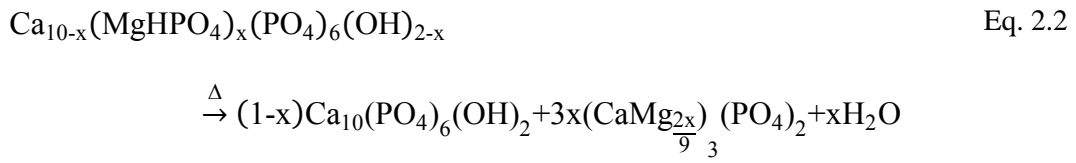
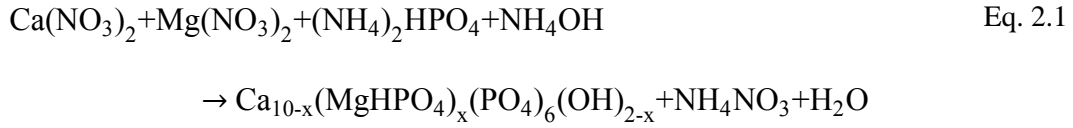
Furthermore, Mg suppresses the β TCP conversion to the undesirable highly-degraded α TCP phase when exposed to high temperatures (Ballouze et al., 2021; Gallo et al., 2019; Kannan et al., 2007; Kumar et al., 2015). The Mg insertion increases the β TCP thermal stability up to 1400°C, which is highly beneficial for

producing porous scaffolds or granules at high temperatures. Lastly, the density and mechanical strength of the BCP scaffolds are further improved by the insertion of the smaller Mg atoms in the β TCP lattice. The Mg insertion causes a contraction in the lattice parameters and improves the densification properties of Mg-BCP (Kannan et al., 2005; Sopyan et al., 2011; Sopyan & Rahim, 2012). In fact, the weak mechanical strength and brittleness are well-known major disadvantages of CaPs, particularly when they are implanted into a load-bearing site raising the risk of fragility fractures with any additional pressure applied (Kannan et al., 2005; Sopyan et al., 2011; Sopyan & Rahim, 2012). Insertion of Mg into the BCP has been proven to significantly improve the mechanical strength of Mg-BCP (Marahat et al., 2020).

2.5 Mg-BCP Synthesis Routes

Table 2.2 summarizes the methods, precursors, and synthesis parameters that were used to synthesize Mg-BCP powders. Generally, Mg-BCP powder is synthesized via the wet precipitation method, the sol-gel method, the gel diffusion method, and the solid-state method (Ballouze et al., 2021). The main chemical precursors used in Mg-BCP synthesis are calcium nitrate tetrahydrate $\text{Ca}(\text{NO}_3)_2 \cdot 4\text{H}_2\text{O}$, magnesium nitrate hexahydrate $\text{Mg}(\text{NO}_3)_2 \cdot 6\text{H}_2\text{O}$, and diammonium hydrogen phosphate $(\text{NH}_4)_2\text{HPO}_4$ as the Ca, Mg, and P sources, respectively (Kannan et al., 2005; Kim et al., 2012; Kubarev et al., 2008; Kumar et al., 2015; Marahat et al., 2019). The synthesis precursors are mixed under vigorous stirring condition until magnesium-doped calcium-deficient hydroxyapatite (Mg-CDHA) $(\text{Ca}_{10-x}(\text{MgHPO}_4)_x(\text{PO}_4)_6(\text{OH})_{2-x})$ precipitate is formed as shown in Equation 2.1 (Ballouze et al., 2021; Kubarev et al., 2008). The precipitate is then aged, washed, separated, and dried. This is followed by a calcination process at a high temperature

in order to decompose the Mg-CDHA to the biphasic mixture of Mg-BCP, as shown in Equation 2.2. Moreover, the calcination process aims to expel the water and other extra phases, including CO⁻² and NO₃⁻² (Ballouze et al., 2021; Basu & Basu, 2019a; Kubarev et al., 2008).



Based on the published reports (Table 2.2), the chemical composition of the resulted Mg-BCP basically depends on the (Ca+Mg)/P ratio and the calcination temperature. The calcination temperature for Mg-BCP ranged between 600°C and 1400°C (Table 2.2). It is worth mentioning that βTCP is not stable and transforms to αTCP at a temperature higher than 1125°C. However, with the Mg insertion, the allotropic conversion of βTCP to αTCP could be delayed to 1400°C (Kannan et al., 2005; Kumar et al., 2015). Moreover, the decomposition of the calcium-deficient hydroxyapatite (CDHA) occurs at around (700°C – 800°C) in the absence of Mg doping. With the Mg substitution, the decomposition of CDHA will occur at a lower temperature (600°C), which is beneficial to the synthesis process. The substitution of the smaller Mg ion into the larger Ca site creates a destabilizing effect in the lattice, and in turn causes the phase transition to occur at a lower temperature (Gozalian et al., 2011; Massit et al., 2020). On the other hand, the (Ca+Mg)/P ratio ranged from 1.42 to 2.00. However, the majority of the published reports maintained this ratio between 1.5 and 1.67, which is between the Ca/P ratio of βTCP (Chemical formula is

$\text{Ca}_3(\text{PO}_4)_2$ where $\text{Ca/P} = 1.5$) and stoichiometric HA (Chemical formula is $\text{Ca}_5(\text{PO}_4)_3(\text{OH})$ where $\text{Ca/P} = 1.67$) (Kannan et al., 2005, 2008, 2009; Kim et al., 2013, 2015; Kim et al., 2012; Marahat et al., 2019). Theoretically, the expected Ca/P ratio in the resulted Mg-BCP powder can be calculated according to Equation 2.3 (Kannan et al., 2009).

$$\text{Expected Ca/P} = \text{wt\% of HA} \times 1.67 + \text{wt\% of } \beta\text{TCP} \times 1.5 \quad \text{Eq. 2.3}$$